Numerical Analysis of Moisture Flow and Concrete Cracking by means of Lattice Type Models

D.Jankovic
Delft University of Technology, Faculty of Civil Engineering and Geo-Sciences, Microlab,
P.O. Box 5048, 2600 GA Delft, The Netherlands

M.Küntz
Universite du Quebec a Montreal, Department of Physics, C.P.8888, Succ.centre ville,
Montreal PQ H3C 3P8 Canada

J.G.M.van Mier
Delft University of Technology, Faculty of Civil Engineering and Geo-Sciences, Microlab,
P.O. Box 5048, 2600 GA Delft, The Netherlands

ABSTRACT: Modelling of fluid-flow and the resulting effects on shrinkage and microcracking by means of a combination of two lattice models are presented. For the moisture transport, a Lattice Gas Automaton (LGA) is adopted since it can effectively model moisture loss, whereas for cracking simulation a Lattice Fracture Model (LFM) is used. The resultant moisture gradients are translated into strains by means of a shrinkage coefficient. Strains yield shrinkage stresses, which are applied as pre-stresses on the sample in order to invoke cracking. The principle of the coupling of two lattice models is explained. Some examples of preliminary analyses on a homogenous lattice and a lattice containing a single large aggregate are presented. Problems and advantages to the approach are debated, and existing gaps in knowledge are indicated.

1 INTRODUCTION

Cement-based materials such as concrete have a very complex structure over many length scales. According to Wittmann (1983), concrete can be modeled at three different length scales: macro, meso and micro. Concrete is a random composite at each scale. At the macro-level, the material is considered as an isotropic continuum (meter scale). At this level full-scale structures are considered. The meso-level operates at the millimeter scale and deals with aggregates, pores, cracks and interfaces, while the micro-level presents the structure of the hardened cement in μm.

Although the "three-level numerical concrete" is widely accepted, it is hardly possible to draw a line among the scales in concrete where to look for the causes of cracks. One of the proposed mechanisms is weakening of the concrete due to differential drying in the early stage of concrete hydration when moisture gradients develop, long before any load is applied. Non-uniform drying causes drying shrinkage, which induces tensile stresses that could be much higher than the low concrete tensile strength and eventually cause cracking (Bisschop & Van Mier 2001).

The drying shrinkage behavior in concrete occurs at different scales: in the sample of 1 m^3 (macro-level) but also at or below the nanometer scale (capillary condensation), which occurs in the "gel" phase of the cement paste (Bentz et al. 1995). Scales are simply incorporated into each other. At the micrometer level, unhydrated cement particles, gel, crystalline hydration and porosity are observed while at the millimeter scale, cement paste, aggregates, and air voids are seen. Only recently drying shrinkage investigations have turned to the microscale and microstructure of the concrete (Xi & Jennings 1992).

The problem starts with the determination of the location of crack initiation. Weakening of the concrete due to differential drying is extreme in highly porous areas such as the porous interface transition zone (ITZ) around the aggregates. The size of the zone is extremely small (10 - 50 μm) and its microstructure has different properties than the rest of the bulk cement paste. Although very small in size, the ITZ is considered to be the weakest part of concrete, where cracking originates. The porosity in the ITZ is large compared to the cement paste (Mindess 1989) which causes low strength in this zone. This confirms that observations should be carried out at very small level (scales), which is rather complicated. Therefore numerical tools may be helpful to elucidate certain phenomena such as structure formation, crack growth and moisture transport (Sadouki & Van Mier 1997).

The aim of the present study is to model fluid (moisture) flow in the interface zone. The problem is highly complex and three-dimensional (3D). At this stage a 2D approach is already quite challenging not in the last place due to computational limitations. Fluid-flow at macro-level is commonly modeled by means of the Navier-Stokes equations under the assumption of continuity. The analytical solution of this equation exists only for very simple geometry.

It certainly does not apply to heterogeneous and complex concrete microstructure (Rothman 1988). A numerical solution is needed, and it was applied through a statistical model for fluid-flow, Lattice Gas Automaton (LGA). In principle, it is possible to include complex microstructure into LGA although more research will be needed before this is accomplished.

The moisture distribution calculated with the LGA serves as a "load" in the subsequent shrinkage analysis and crack growth simulations with the existing lattice fracture model. Differential moisture distributions lead to differential shrinkage, which in turn leads to differential strains and cracking. The problem to be resolved is to develop a realistic coupling among the LGA model for moisture flow, material structure, shrinkage and a mechanical model for crack growth.

2 LATTICE MODELS

2.1 Lattice Gas Automaton

A Lattice Gas FHP model, named after the authors Frisch, Hasslacher & Pomeau (Frisch et al. 1986, 1987) is applied for "numerical" moisture flow since the microscopic behavior of this lattice is very close to the Navier-Stokes equations for incompressible fluids at the macroscopic scale. LGA has been selected for its application to single and multiphase flows in irregular geometries with accompanying chemical reactions i.e. exactly what processes in the ITZ (Rothman 1988).

A cellular automaton is basically a computer algorithm that is discrete in space and time and operates on a lattice of sites. The class of cellular automata that can model hydrodynamics is called Lattice Gas Automaton. Lattice gas cellular automata are special kind of gas with discrete velocity, in discrete time and space in which identical particles move on the lattice from one site to the other. Although with some drawbacks such as statistical noise and exponential complexity, these are the mathematical models for systems in which many simple components act together and produce complicated behavior patterns. Instead of solving Navier-Stokes equations directly, lattice gas cellular automata are introduced as polynomial approximation.

The connection between the macro and micro world is through density (ρ) and momentum (ρu). They can be replaced by the average number of particles per node $\rho = \sum N_i$ ($N_i = d/7$, $0 \leq i \leq 6$) and momentum $\rho u = \sum N_i c_i$ where c_i is a velocity per node ($c_i = cos[1/3\pi i]$, $sin[1/3\pi i]$). The density affects the flow of the fluid. Due to the difference in the densities between the nodes, particles propagate and collide (Frisch et al. 1986) following,

$$\nabla u = 0 \tag{1}$$

$$\rho \frac{\partial u}{\partial t} = -\rho(u * \nabla)u - \nabla p + \mu\nabla^2 u \tag{2}$$

where u = the velocity; ρ = density; p = pressure; and μ = viscosity.

2.2 Numerical modeling by LGA

LGA is a simple, regular, triangular (hexagonal) mesh (Fig. 1a) where particles propagate and collide with each other according to a certain collision rule (Frisch et al. 1987). The collision rules depend on the type of lattice gas model.

In the present case, a 7-bit FHP model (FHP III) is used with collision rule FHP5. The most important characteristic of this model is the maximum of seven fluid particles that rests at each lattice node. Six can move in any of six directions (Fig. 1b) with a unit speed while the seventh is always at rest having zero velocity. Beside these so-called fluid particles, solid particles are present as well. They can be randomly distributed in the lattice in a certain percentage or concentrated at a certain area in the lattice. Their location does not coincide with the location of the fluid particles.

The collision rules will be different for the collision of two or three fluid particles or if one fluid particle collides with a particle at rest. Collision between a fluid and a solid particle or solid boundary will be considered as a boundary condition. The size of the lattice is given by Xsize and Ysize. This is adopted as the size of the imaginary sample. The considered problem is drying of the sample. The LGA model has been adopted from previous saturation model (Küntz et al. 2001) which was modified for drying simulations.
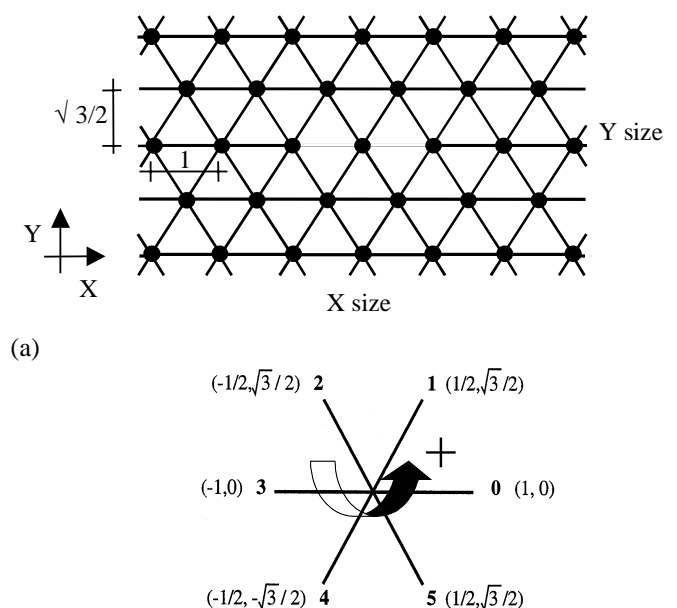

(a)

(b)

Figure 1. (a) Lattice Gas Automaton, FHP model, (b) movement of the particles with velocities (c_i) in six directions.

In the LGA program, the modifications also included the presence of the aggregate (single or more aggregates inside the sample). The initial density is equal to 0.9. Drying is applied by assigning a density 0.2 on the left side as presented in Figure 2.

Boundary conditions are periodic (by default) along the top and bottom, considering that particles exit on one side and enter on the other. Periodic boundaries help to eliminate artificial edge effects typically present in a small-scale model (Bentz et al. 1993). Periodicity is broken on the left side, introducing a barrier. The boundary condition, which is a specific collision rule, exists among fluid and solid surface. It is possible to recognize two extreme collision rules: specular or bounce-back reflection, depending on the surface. Specular is a reflection on a perfectly smooth surface while bounce-back is a reflection on a rough surface (Lavallee et al. 1991). The present boundary condition is expressed with the ratio r = specular/bounce-back (r = 1 for specular and r = 0 for bounce-back reflection).

Two main numerical analyses will be presented here. One deals with the homogeneous material only and in the other a single aggregate is present in the middle to simulate an obstacle in the flow.

2.3 LGA results

The first analysis simulates drying of a homogeneous sample. Two boundary conditions were applied, r = 1 and r = 0. The initial wet stage is the same for both cases (Fig. 3a). After a certain number of iterations or time steps in the program (90,000) drying of the sample is visible (Figs 3b, c). Different boundary conditions have an effect on the drying process (Fig. 4). In the second analysis a solid obstacle in the form of an aggregate was placed in the middle. Since the solid particles are mostly concentrated in the middle forming an aggregate, the moisture is lost more quickly (the number of "fluid" particles rapidly decreases). The result is that the sample is dried out after 15,000 steps.
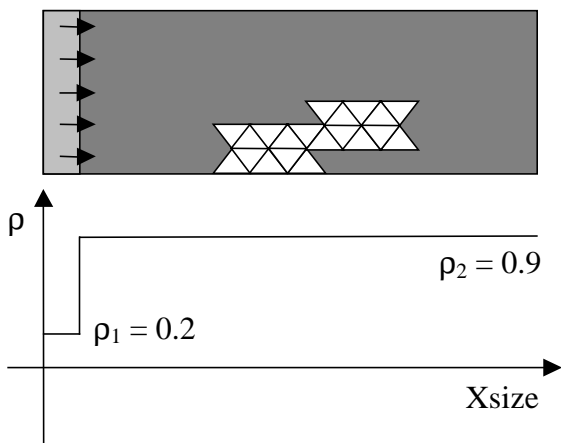

Figure 2. Schematic presentation of LGA model with the distribution of densities at the initial stage.
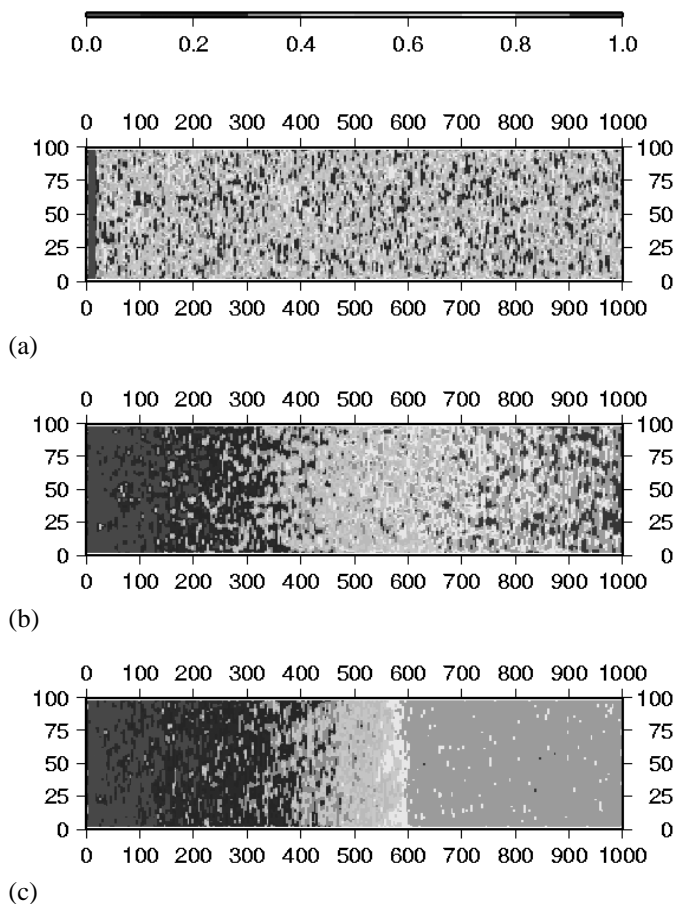

(a)

(b)

(c)

Figure 3. (a) Initial wet stage, (b) dried sample after 90,000 iterations (r = 1), (c) dried sample after 90,000 iterations (r = 0).

Different boundary conditions were applied: r = 0 and r = 1 (Fig. 6).

2.4 Drying profiles

The drying process can be followed from the drying profiles. The calculation was made along the Xsize of the lattice taking into account the average density value of every point along the height of the sample. The two profiles in Figure 4 present the analysis with r = 1 and r = 0 boundary condition. Drying profiles with specular-reflection (r = 1) show great rate of the particle loss after first 5000 steps. As the number of iteration increases, the moisture gradient decreases and leads to the dried sample with equally distributed moisture content of 0.2. Bounce-back boundary condition showed a larger moisture gradient after first 5000 steps. This means that the shrinkage cracking is dangerous only in the first stage.

Later on the moisture loss is slower, and the complete dried stage has not been reached after 90,000 steps. Drying profiles for the "single aggregate" sample gave a rather irregular picture which could be interpreted as an insufficient size of the LGA. The real comparison of the numerical results should be made with the experimental results (Fig. 5). The moisture losses are related to time (t). This is presented in Figure 5a. The results from the LGA show similar relation as in the experiments (Fig. 5b)
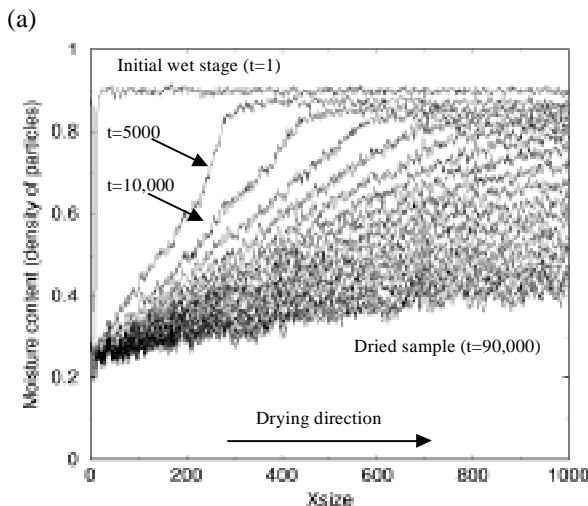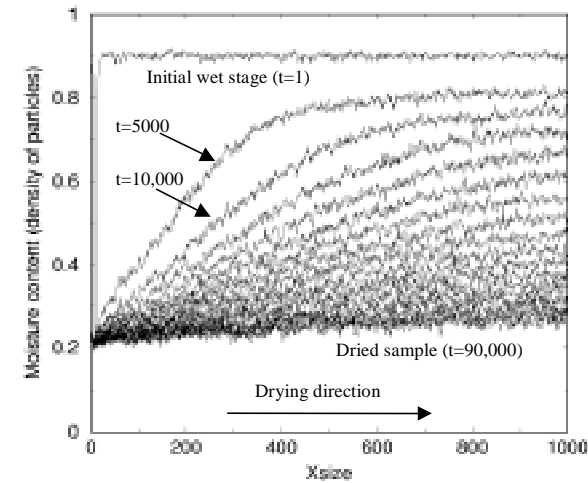
(a)

(b)

Figure 4. Density profiles due to drying at different time steps for (a) r = 1, (b) r = 0.

but the comparisons could not be made completely. The size and time scale of the lattice gas "sample" are still unknown and consequently could not be compared to the size of the sample and the time in the experiments.

2.5 *Lattice Fracture Model (LFM)*

The existing Lattice Fracture Model (Schlangen & Van Mier 1992) has been used for the fracture analysis. For the "drying" analysis, certain modifications have been done as explained in this section. The lattice fracture model was chosen because of its good capabilities to simulate crack-patterns due to tensile mechanical loading. An equivalent beam (Fig. 7) of the lattice frame replaces the continuum.

In the DIANA version of the lattice, two types of elements need to be defined in order to run fracture analyses: beam and continuum elements. Beam elements are only applied in the area where the cracks are expected. The lattice fracture model has the same geometry as the FHP lattice gas since they are both presented by a regular triangular mesh. In the lattice fracture model, triangles are constructed from beam elements. Heterogeneity can be modeled through an

appropriate statistical distribution of strength and stiffness values assigned to the beam elements or by superimposing a particle structure of concrete and assuming properties according to the material phase in which they are located. A linear-elastic, purely brittle fracture law is adopted in the model. When a beam "cracks", it is instantaneously removed from the mesh.

3 COUPLING THE TWO LATTICE MODELS

3.1 *Background*

The main reason for the coupling analysis is to allow for crack growth in concrete interface zone due to moisture flow and using the mesh similarities of both models. Shrinkage and crack growth are considered before the application of any mechanical load.

3.2 *Comparison of the two lattice models*

The two lattice models can be combined due to their similarities, such as the same mesh geometry (Figs 1, 9) and the same load application (at the nodes). Having the same triangular shape, the function of lattice connections between each two nodes is different for each model. In the case of LGA, lattice connections are there just to provide a path for the particles to move. The propagation is done with ima-
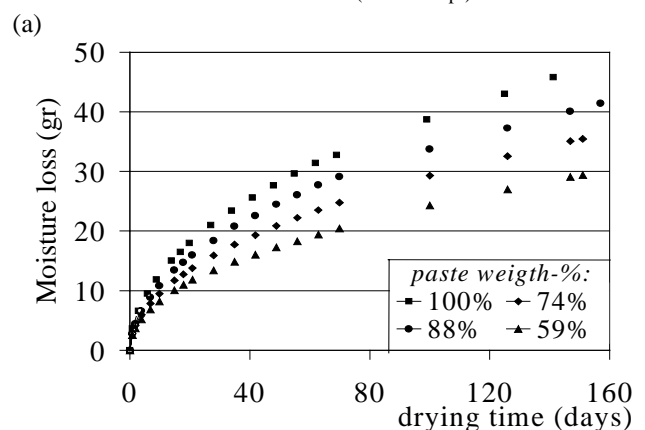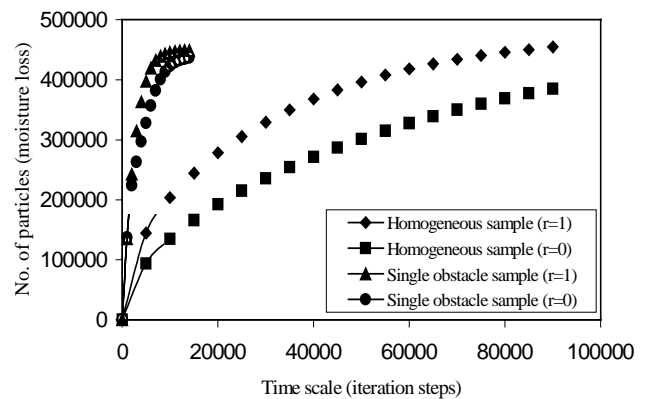

(a)

(b)

Figure 5. Moisture loss as a function time, (a) numerical analysis, (b) experimental results (Bisschop & Van Mier 2001).
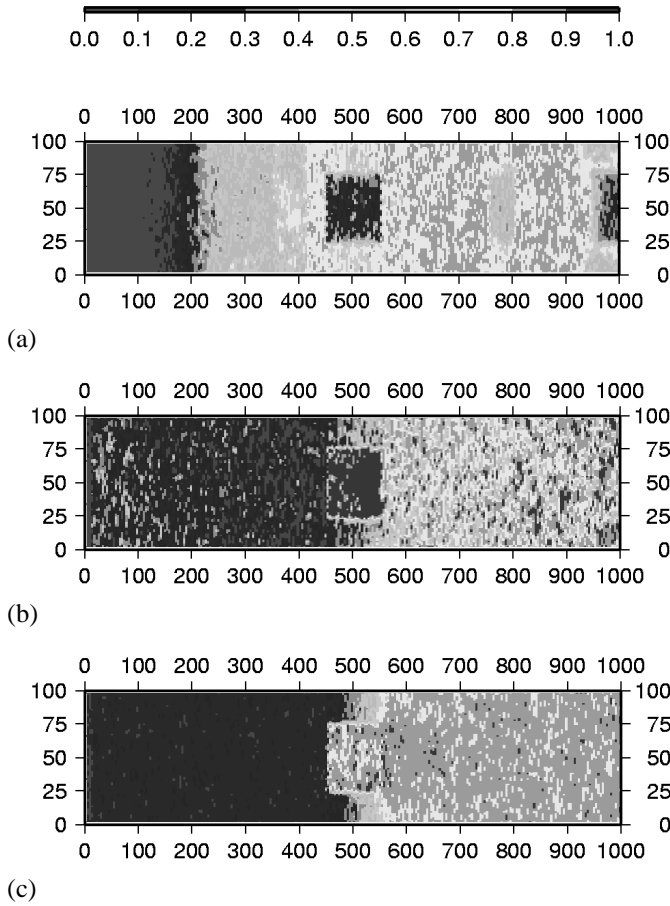
234

(a)

(b)

(c)

Figure 6. Example with single aggregate in the middle (a) wet stage after 400 iterations (r = 0). Drying simulation (b) after 3000 iterations (r = 1), and (c) after 3000 iterations (r = 0).
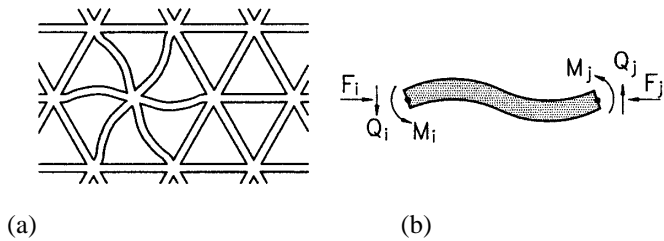

(a)   (b)

Figure 7. (a) Regular triangular lattice of beam elements, (b) external forces and deformations of a beam (after Schlangen, 1993).
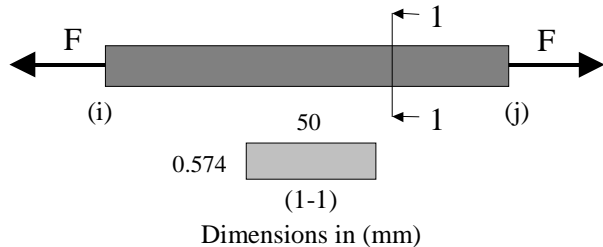

Figure 8. Applied prestress load to a beam element.

ginary ticks of a clock from one node to the other (on a unit-length path). Particles move with a unit speed such that momentum and mass are conserved. In the Lattice Fracture Model nodes are connected by beam elements with specified properties.

Changes in these properties can influence the calculated stress and strain, and accordingly the fracture process. Both models are two-dimensional with the specified boundary conditions but in principle, extension to 3D is possible.

3.3 Coupling

The LGA analysis is performed on a relatively fine lattice. However, to reduce computational effort, the moisture content was calculated for every block of 8 x 8 nodes in the LGA. Subsequently the fracture lattice was projected such that the nodes coincided with the centers of these blocks.

The computation proceeds as follows. First the moisture content (density h) is calculated with the LGA at each node. The density values at these points were used for the determination of the density gradients between each two nodes (Δh). After the calculation of Δh, the shrinkage strain ε_{sh} was calculated as well as shrinkage stress σ_{sh} following:

$$\varepsilon_{sh} = \alpha_{sh}\Delta h \qquad (3)$$

$$\sigma_{sh} = \varepsilon_{sh}E \qquad (4)$$

where α_{sh} = drying shrinkage coefficient (0.003); ε_{sh} = shrinkage strain; E = Young's modulus (25,000 MPa); σ_{sh} = shrinkage stress (MPa). The same equations for shrinkage strain and stress as well as the element properties (α_{sh}, E) were used by Sadouki & Van Mier (1997) in a continuum-based approach.

In LFM the load must be specified for each element as force (F) and moment (M). Consequently a simple axial force (Eq. 5 & 6) derived from the shrinkage stress is applied to each beam (Fig. 8) on both nodes (i, j) as follows:

$$F = \sigma_{sh}A \qquad (5)$$

$$M = 0 \qquad (6)$$

where A = cross-sectional beam area. As a subroutine in the LGA, the nodal densities are used to calculate nodal forces and moments, which serve as input for the LFM.

In the fracture lattice, the meso-structure of concrete is included. Three material phases are normally distinguished with aggregate, matrix and bond beams. In the first analysis, meso-structure has been omitted and a lattice with homogeneous elastic properties is considered (Fig. 9a). Continuum elements are placed on the top and bottom for the symmetry. The cracks are expected only in the area of the beam elements. The whole specimen was supported in y direction with the exception of the nodes at the right end which were supported in both x and y direction. Heterogeneity is simulated in the second example with a single aggregate model (Fig. 9b).
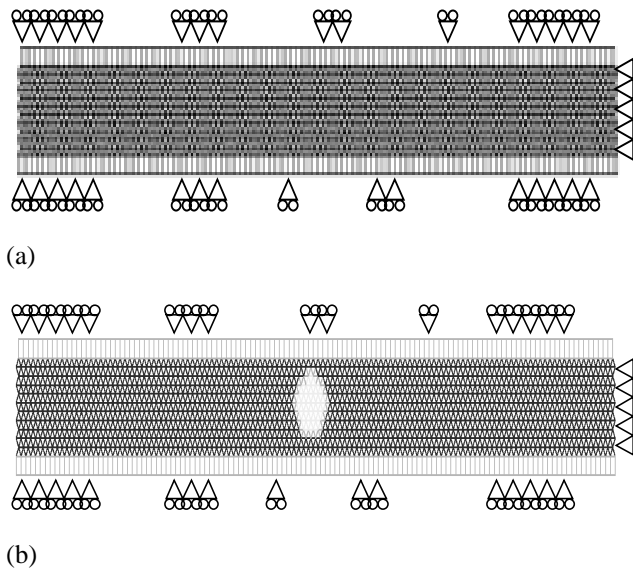
(a)

(b)

Figure 9. Lattice Fracture Model: mesh with the supports (continuum elements supported on top/bottom), (a) homogeneous structure (b) with single aggregate in the middle.

4 RESULTS AND DISCUSSION

4.1 *First example: homogeneous lattice*

A small percentage of solid particles (3%) was present in the LGA. The solid particles were scattered randomly in the sample. LGA analysis was made with 90,000 steps (iterations), which was sufficient to follow the changes of the moisture flow in the specimen. Two limit boundary cases were taken into consideration: r = 0 and r = 1.

In the present example, the lattice fracture model was considered to be homogeneous (all beams are given the same properties). For an applied load, only a single step was made in the fracture analysis. The size of the LFM mesh was 125 x 12, which was decreased for the computational reasons from 1000 x 100 in the LGA.

In Figure 10, the crack pattern is shown. The way that cracks will develop depends on the fracture law that is implemented in Lattice Fracture Model. At this moment the fracture law is convenient for mechanical loading in tension where realistic crack patterns are simulated. Under mechanical loading, the analysis runs always with a unit load and the stress in each element is calculated. The critical element i.e. the element that has the highest stress, relative to its strength (Schlangen & Van Mier 1992) is removed at each step.

With the moisture load from different LGA steps, the crack pattern (Fig. 10) will not be continuous since for every new LFM step, another moisture load is taken from LGA. As a consequence, elements will crack randomly in the area that dries out first.
In the given example, the drying starts from the left side. The gray-scale of the sample changes from the left to the right symbolizing drying (lower RH) on

the left side. If the same step from LGA would have been taken and used as input load for many fracture steps (not only once) then the crack pattern would be more continuous. Note that the LGA noise leads eventually to discontinuous cracking. In addition, the fracture law might affect the results.

A number of additional remarks should be made on the LGA itself. The fracture results depend on the number of steps after which the results have been saved. If the step is bigger, more fluid particles will be "lost" in the drying process, which corresponds to faster drying. In the first example LGA moisture results are saved after every 5000 steps (Fig. 10a) and the results from every 5000 steps were used for one step in LFM. This means that at every new step in LFM, a new "moisture" load is taken. The important question is if a certain number of LGA steps could produce the most critical cracking pattern and what the number of these steps would be. The present model does not yield a solution. The cracks develop at random locations in the model, depending on the
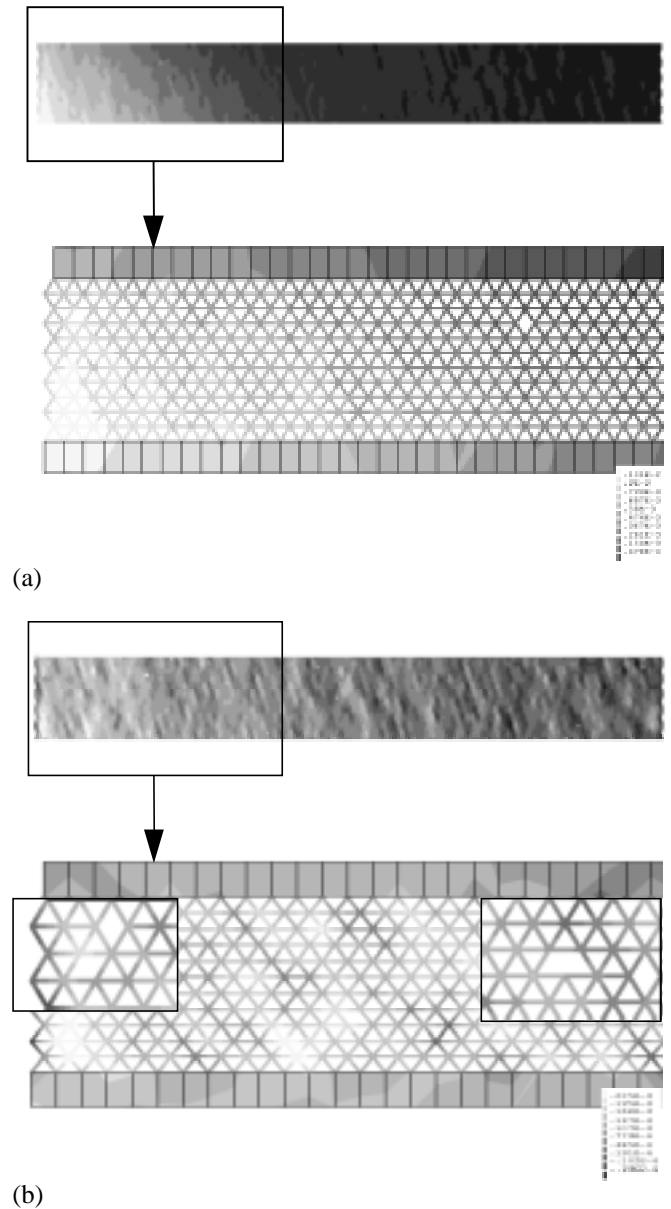

(a)

(b)

Figure 10. Deformations and cracks in LFM, (a) after 5000 steps in LGA for r = 1, (b) after 90,000 steps in LGA, r = 1.

236

moisture gradients. After 90,000 LGA time-steps, cracks were found spread over the complete sample (Fig. 10b).

4.2 Second example: lattice containing a single obstacle in the middle

Lattice gas simulations have been done with a single aggregate placed in the center of the LGA (Fig. 6). The percentage of the present solid particles was 0.8% such that all-solid particles were concentrated in the middle, forming a big particle. The presence of the great concentration of solid particles and the adopted bounce-back boundary conditions ($r = 0$) accelerated the drying process, so there was no need to save LGA results every 5000 steps. Only 1000 steps were sufficient. Figure 11 shows the moisture movement (by gradual changes in gray-scale) and the crack pattern. Three-phase material was used in the lattice fracture model by giving different strength
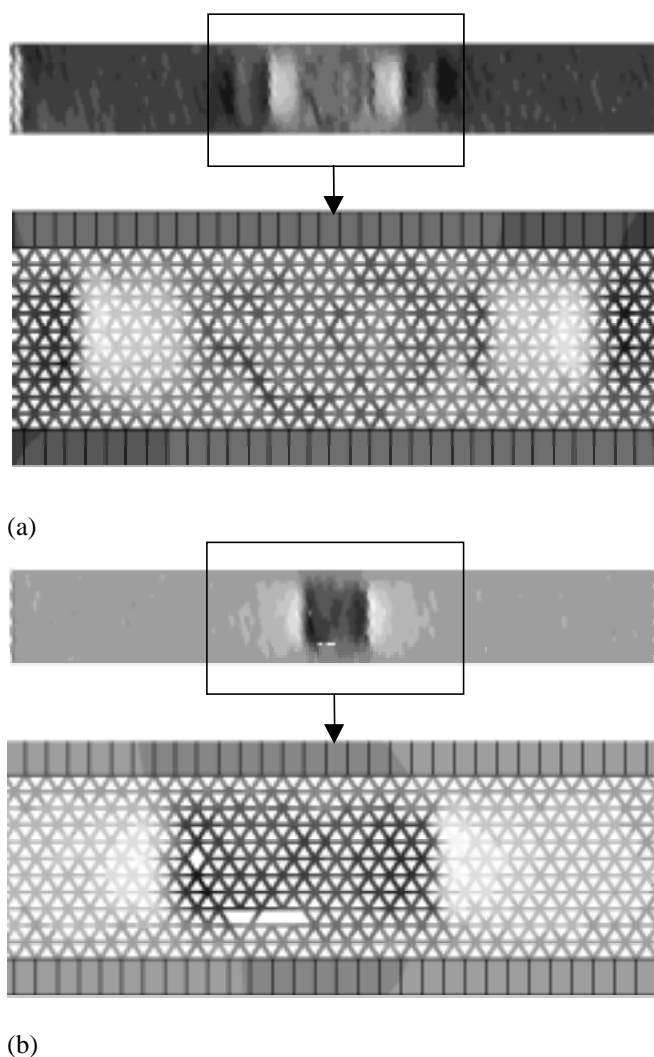
(a)

(b)

Figure 11. Deformations and cracks in LFM, (a) after 1000 steps in LGA, $r = 0$, (b) after 15,000 steps in LGA, $r = 0$.

values for every phase with the lowest values in the interface zone around the aggregate. Only 15,000 steps were sufficient to obtain a completely dried specimen. Cracking started to develop randomly at the left side and then propagated in the ITZ, around the aggregate.

5 CONCLUSION

A cellular automata lattice gas FHP III model was used to analyze the moisture flow in porous media. It is a very simple method derived from statistical physics, which could give the complicated pattern of moisture behavior in porous concrete.

The results show that it is possible to combine two different methods: lattice gas automaton (LGA) and fracture lattice analysis (LFM) taking into account their similarities and overcoming the differences. A number of drying simulations were carried out on homogeneous samples and samples containing a single large aggregate. The flow around the aggregate was clearly blocked, and future research should focus on the typical collision rule and/or boundary condition for flow around the aggregate.

Different boundary conditions were used in LGA: specular reflection and bounce-back expressed as a ratio r = specular/bounce-back. They describe the behavior of the fluid particles after collision with the solid particles and the boundaries. In the first example, the analysis with specular-reflection speeds up the drying process in comparison to the bounce-back boundary condition. On the other hand, the bounce-back boundary condition gives higher moisture gradients in the first steps and thus larger shrinkage strains, which causes more cracks at the left side.

The cracking patterns in the LFM will depend on the applied boundaries. In the first example, with the homogeneous structure, cracks appear in the whole sample, starting from the driest part on the left. In the second example, cracking is mostly concentrated around the aggregate. The obtained moisture loss vs. time curves compares well to the results obtained recently in one-dimensional drying experiments. These experiments will be used in the future research to scale the time in the simulations.

The fracture process in the LFM has to be reformulated. In particular addressing to the time-scales needed for the appearance of drying shrinkage cracks is considered essential.

ACKNOWLEDGEMENT

REFERENCES

Bazant, Z.P. & Najjar, L.J. 1971. Drying of concrete as a non-linear problem. *Cement and Concrete Research* (1): 461-473.

Bentz, D.P., Garboczi, E.J. & Coverdale, R.T. 1993. Computational materials science of cement-based materials: An education module. *United States Department of Commerce, Technology Administration, National Institute of Standards and Technology, NIST Technical Note* 1405.

Bentz, D.P., Quenard, D.A., Baroghel-Bouny, V., Garboczi, E.J. & Jennings, H.M. 1995. Modelling drying shrinkage of cement paste and mortar: Part 1. Structural models from nanometers to millimeters. *Materials and Structures* 28: 450-458.

Bisschop, J. & Van Mier, J.G.M. in press. The effect of aggregates on drying shrinkage microcracking in cement-based materials. *Con. Sci. Techn*.

Bisschop, J., Pel, L. & Van Mier, J.G.M. in press. Effect of aggregate size and paste volume on drying shrinkage microcracking in cement-based composites. *Proceedings ConCreep-6*.

Frisch, U., Hasslacher, B. & Pomeau, Y. 1986. Lattice-gas automata for the Navier-Stokes equation. *Physical Review Letters* 14(56): 1505-1508.

Frisch, U., d'Humieres, D., Hasslacher, B., Lallemand, P., Pomeau, Y. & Rivet, J-P. 1987. Lattice gas hydrodynamics in two and three dimensions. *Complex Systems* 1: 648-707.

Jankovic, D. 2000. *Moisture Flow and Microstructure Development of the Interface Zone*. Report, TU Delft, Faculty of Civil Engineering and Geo-science. CM2000-010.

Küntz, M., Van Mier, J.G.M. & Lavallee, P. in press. A lattice gas automaton simulation of the non-linear diffusion equation: a model for moisture flow in unsaturated porous media. *Transport in Porous Media*.

Lavallee, P., Boon, J.P. & Noullez, A. 1991. Boundaries in lattice-gas flows. *Physica D* 47: 233-240.

Mindess, S. 1989. Interfaces in concrete. In Jan P. Skalny (ed.), *Materials Science of Concrete* I: 163-180. Westerville: The American Ceramic Society, Inc.

Rothman, D.H. 1988. Cellular-automaton fluids: A model for flow in porous media. *Geophysics* 53(4): 509-518.

Rothman, D.H. & Zaleski, S. 1997. *Lattice-gas Cellular Automata; Simple Models of Complex Hydrodynamics*. Cambridge: UK Cambridge University Press.

Sadouki, H. & Van Mier, J.G.M. 1997. Meso-level analysis of moisture flow in cement composites using a lattice type approach, *Materials & Structures* 30(204): 579-587.

Schlangen, E. & Van Mier, J.G.M. 1992. Experimental and numerical analysis of micro-mechanics of fracture of cement-based composites. *Cem. & Conc. Composites* 14(2): 105-118.

Schlangen, E. 1993. Experimental and numerical analysis of fracture processes in concrete. Ph.D. Thesis. Delft University of Technology, the Netherlands.

Van Mier, J.G.M. 1997. *Fracture Processes of Concrete*. Boca Raton: CRC Press.

Wittmann, F.H. 1983. *Fracture Mechanics of Concrete*. Elsevier Science Publishers.

Wolfram, S. 1986. Cellular automaton fluids 1: basic theory. *Journal of Statistical Physics* 45: 471-526.

Xi, Y. & Jennings, H.M. 1992. Relationships between microstructure and creep and shrinkage of cement paste, *Material Science of Concrete* III: 37-69. American Ceramic Society.